The Impact of Fission on R-Process Calculations

M Eichler[1], A Arcones[2], R Käppeli[3], O Korobkin[4], M Liebendörfer[1], G Martinez-Pinedo[2], I V Panov[5], T Rauscher[6,1], S Rosswog[4], F-K Thielemann[1], C Winteler[7]

[1] Department of Physics, Basel University, Klingelbergstrasse 82, 4056 Basel, Switzerland
[2] Institut für Kernphysik, Technische Universität Darmstadt, Schlossgartenstrasse 2, D-64289 Darmstadt, Germany
[3] Seminar for Applied Mathematics, ETH Zürich, Rämistrasse 101, 8092 Zürich, Switzerland
[4] Astronomy and Oskar Klein Centre, Stockholm University, AlbaNova, SE-10691 Stockholm, Sweden
[5] Institute for Theoretical and Experimental Physics, Bol'shaya Cheremushkinskaya ul. 25, Moscow, 117259 Russia
[6] Centre for Astrophysics Research, School of Physics, Astronomy and Mathematics, University of Hertfordshire, Hatfield AL10 9AB, UK
[7] Institut Energie am Bau, Fachhochschule Nordwestschweiz, St. Jakobs-Strasse 84, 4132 Muttenz, Switzerland

Abstract. We have performed r-process calculations in neutron star mergers (NSM) and jets of magneto-hydrodynamically driven (MHD) supernovae. In these very neutron-rich environments the fission model of heavy nuclei has an impact on the shape of the final abundance distribution and the second r-process peak in particular.
We have studied the effect of different fission fragment mass distribution models in calculations of low-Y_e ejecta, ranging from a simple parametrization to extensive statistical treatments (ABLA07).
The r-process path ends when it reaches an area in the nuclear chart where fission dominates over further neutron captures. The position of this point is determined by the fission barriers and the neutron separation energies of the nuclei involved. As these values both depend on the choice of the nuclear mass model, so does the r-process path. Here we present calculations using the FRDM (*Finite Range Droplet Model*) and the ETFSI (*Extended Thomas Fermi with Strutinsky Integral*) mass model with the related TF and ETFSI fission barrier predictions. Utilizing sophisticated fission fragment distribution leads to a highly improved abundance distribution.

1. Introduction

The r-process (*rapid neutron capture process*) is responsible for the production of about half of the heavy elements in our universe. Although the astrophysical site is still unknown, the physical requirements point towards explosive environments. Possible scenarios include core-collapse supernovae and neutron star mergers. The r-process reaction path in the nuclear chart proceeds in the very neutron-rich, unstable region, thus involving nuclei that cannot (yet) be studied in experiments. This means that r-process reaction networks need to rely on theoretically predicted nuclear data.
When the material reaches the top end of the reaction path, fission becomes a dominant decay channel (either via spontaneous fission for very low fission barriers or via delayed or induced fission, if beta-decays or neutron captures produce compound nuclei above their fission barrier energies). Then nuclei split into two lighter ones with roughly half the mass of the parent nucleus, while there is a possibility of several fission neutrons to be emitted. While the number of fission neutrons has been measured to be

2 – 4 for experimentally studied nuclei, it is known to increase with mass number and $\beta-$decay energy of the mother nucleus [1]. If the neutron density is still high enough, the freshly made daughter nuclei continue capturing neutrons, thus keeping the r-process alive. In that sense, a fission reaction increases the amount of seed nuclei during the event. Obviously, a realistic description of fission processes are just as important as other nuclear reactions in r-process calculations. However, since fission reactions do not only need a prediction of the reaction rate but also of the fission products, fission treatment is more complex.

The fission probability of a nucleus is directly dependent on the fission barrier, which is a feature predicted by the nuclear mass model. Therefore, the mass model determines the end of the r-process path, having a direct influence on the final abundance distribution.

The mass number and proton number of the daughter nuclei that are produced in a fission reaction are given statistically by fission fragment distribution models. These models are usually fitted to known fission data and vary in complexity.

2. Method

We have tested the impact of two different nuclear mass models and four fission fragment distribution models on the final abundances for both a neutron star merger scenario [2,3] as well as a magneto-hydrodynamically driven supernova [4]. Our nucleosynthesis calculations have been done using the nuclear network WINNET [4], closely following the descriptions in [3] (NSM) and [4] (MHD supernova), respectively. This way, a direct comparison to these works can be made. A more detailed description of the nuclear network and the procedure can be found in the two papers indicated.

The two mass models are the *Finite Range Droplet Model* (FRDM) [5] and the *Extended Thomas Fermi with Strutinsky Integral* (ETFSI) [6] with the related TF [7] and ETFSI [8] fission barrier predictions. These are mass models for which a complete set of data exist in order to perform elaborate r-process

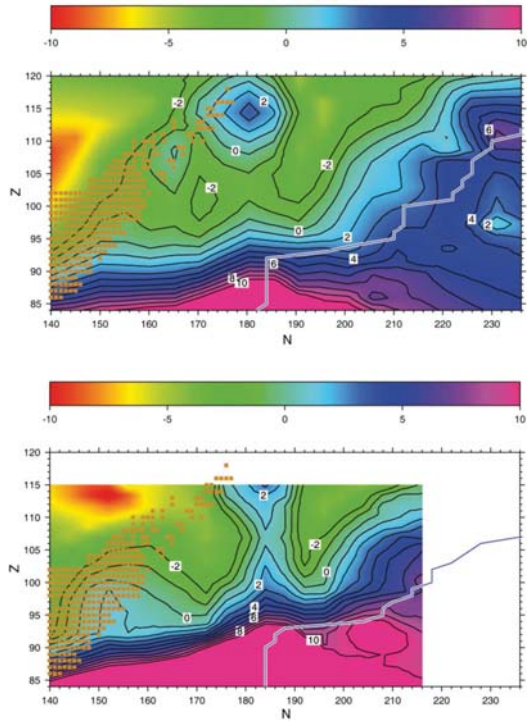

Figure 1: The quantity $B_f - S_n$ at the heavy-mass end of the nuclear chart for the FRDM (top) and the ETFSI (bottom) mass models. See text for discussion. Figure taken from [9].

calculations. Figure 1 shows contour plots of the quantity $B_f - S_n$ (fission barrier minus neutron separation energy) for both mass models. This quantity determines the dominant reaction (or decay) channel in any particular region in the nuclear chart. If along the reaction path this value is close to 0 MeV or negative, fission will dominate over the (n, γ)- or (γ, n)-reactions and the reaction path will end here. It can be seen from Figure 1 that for the FRDM model the quantity $B_f - S_n$ is not larger than 2 MeV even at the drip line for nuclei with $N \geq 184$, preventing the production of heavier nuclei. The ETFSI model, on the other hand, predicts larger fission barriers along the drip line, thus enabling the reaction path to continue beyond $N = 184$. This means that in calculations employing the ETFSI model the fissioning nuclei are heavier, resulting in heavier fission products.
The fission fragment distribution models we use differ in complexity. They predict the fission products and the number of fission neutrons of each fission reaction using a statistical distribution, accounting for nuclear shell effects. The four models are: (a) Panov et al. (2001) [10], (b) Kodama & Takahashi (1975) [11], (c) Panov et al. (2008) [12] and (d) ABLA07 (Kelic et al., 2008) [13]. Figure 2 demonstrates the

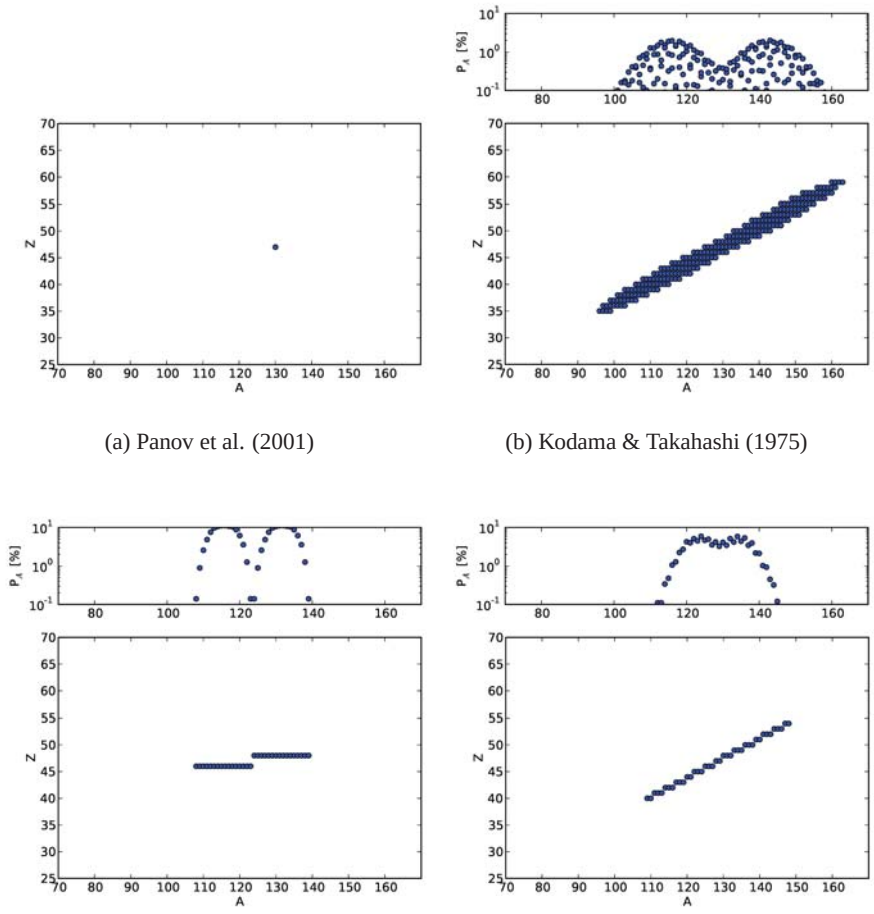

(a) Panov et al. (2001) (b) Kodama & Takahashi (1975)

(c) Panov et al. (2008) (d) ABLA07

Figure 2: Comparison of the four different fission fragment distribution models on the example of a fissioning ^{260}Pu nucleus. Note that the Panov et al. (2001) distribution has only one fission channel per reaction, therefore the probability is always 100%. Calculations using all four models are presented in section 3.

differences of the four models on the example of the fission of ^{260}Pu. The lower part of each graph shows the distribution of the fission products in the nuclear chart, while the upper part marks the probability in percent for each fission channel.

3. Results

We have run r-process calculations testing all the models that have been introduced in the previous section and their differences regarding the final abundance distribution. Two different possible r-process scenarios have been employed: (a) a merger of two neutron stars (NSM) with 1.4 $M_\odot$ each [3], and (b) the neutron-rich jets of a magneto-hydrodynamically driven (MHD) supernova [4]. It has been shown that in both models r-process material is synthesized. However, there is a significant difference: While the electron fraction for the neutron star merger is very low (around $Y_e \approx 0.02 - 0.05$), which allows for several fission cycles before the r-process freeze-out, its value is between 0.2 and 0.4 in the MHD jets. This results in only one fission cycle, taking place around the time of the r-process freeze-out.
Figures 3 and 4 demonstrate the effect of the fission fragment distribution model on the final abundances in an NSM and an MHD supernova scenario, respectively.

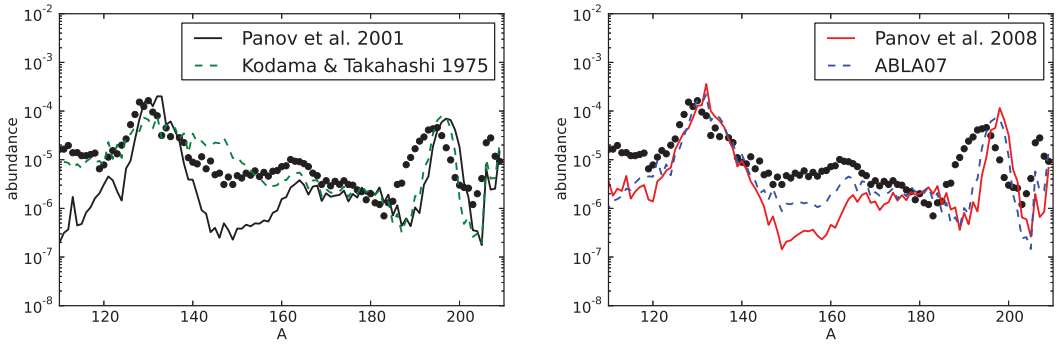

(a) (b)

Figure 3: Final abundances around the second and third peak for a NSM [3] employing four different fission fragment distribution models. For reasons of clarity the results are presented in two graphs. The black dots represent the solar r-process abundances [14]. The mass model is FRDM in all calculations.

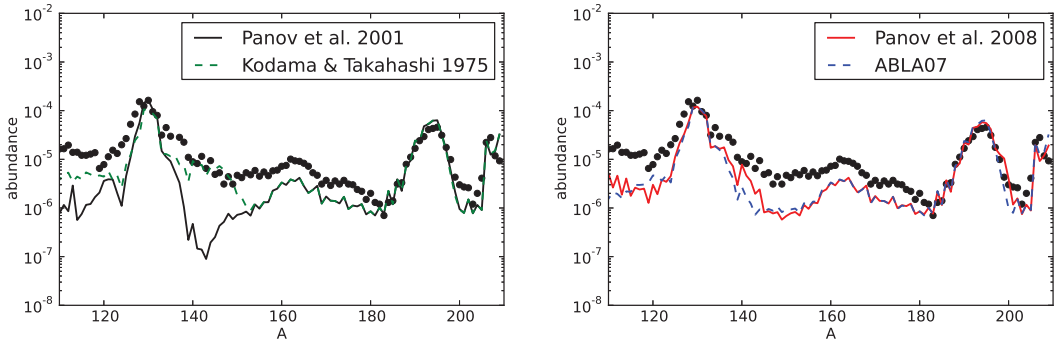

(a) (b)

Figure 4: Same as Figure 3, but for an MHD supernova [4].

The features of the models are clearly visible around the second peak (A $\approx$ 130). The Panov 2001 model produces a very pronounced peak, followed by a sharp drop in abundances. NSM calculations using the Kodama & Takahashi distribution on the other hand do not cause a well-pronounced peak, with the distribution overestimating the production of nuclei with mass number A = 140 – 150, and also the MHD simulations show an unusual abundance pattern. The Panov 2008 and ABLA07 models tend to agree better with the solar abundances, both in terms of shape of the second peak as well as the abundances of the nuclei beyond the peak.

We find that the choice of the nuclear mass model has a smaller impact on the final abundances than the fission fragment distribution model. As already mentioned above, the ETFSI model tends to predict larger fission barriers, allowing the reaction path to run up to heavier nuclei. As the nuclei reach the end of the reaction path and undergo fission, they produce heavier daughter nuclei. Therefore the abundance distribution features heavier nuclei compared to the FRDM model. Figure 5 shows the difference between the two mass models, again for both NSM and MHD supernova scenarios.

A reoccurring feature of NSM calculations is the position of the third peak, which is shifted towards higher masses compared to the solar abundances. This phenomenon has been present in calculations of various authors. We have found that the position of the peak depends on the characteristics of the r-process freeze-out. In particular, neutron captures are still in competition with photodisintegrations after the freeze-out. Therefore, neutron density and temperature are crucial for the further nucleosynthesis processes. A relatively high neutron density and low temperature will result in several neutron captures on heavy nuclei, causing the abundance distribution to shift towards higher masses. This effect can be prevented if the temperature is higher at freeze-out, e.g., if the freeze-out happens earlier. Temperatures of around 1 GK or higher are sufficient for photodisintegrations to effectively compete against the neutron captures, decreasing the average mass number of the heavy nuclei. The second peak material at that time consists to a considerable degree of freshly made fission products. Those are neutron-rich themselves and do not capture additional neutrons. Therefore the second peak does not experience the same shift as the third peak. As a test, we have artificially increased the $\beta-$decay rates for all nuclei with charge number Z $>$ 80 by a factor of 10. This includes the $\beta-$decays which are followed by spontaneous neutron emission. As a consequence, the reaction flow is accelerated and the r-process freeze-out takes place earlier, i.e., at a higher temperature (Figure 6a). The photodisintegrations act against the neutron captures and prevent the shift in heavy nuclei abundances. The rare earth elements (140 $\leq$ A $\leq$ 185) are also affected.

The above example is only one of several ways of preventing the shift in abundances. Another possibility is to decrease the neutron density after freeze-out, e.g., by increasing the (n,γ) and (γ,n) rates.

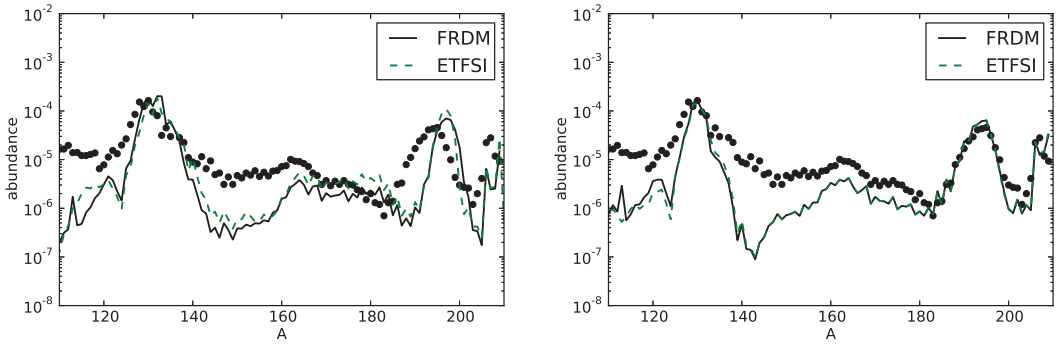

(a) NSM (b) MHD jets

Figure 5: ETFSI mass model (green dashed line) compared to the FRDM model (black solid line) for the NSM scenario (a) and the jets of a MHD supernova (b).

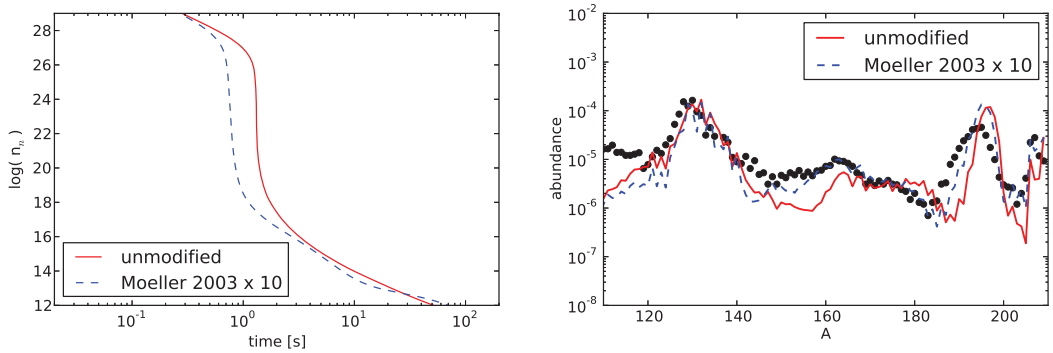

(a) neutron density n_n (b) abundances Y_i

Figure 6: The effect of accelerated $\beta-$decays of nuclei with Z > 80 on the neutron density evolution (a) and final abundances (b). The sharp drop in neutron density marks the r-process freeze-out. In this calculation the mass model is FRDM and the fission fragment distribution follows the ABLA07 prescription. See text for further explanations.

4. Conclusion

We have shown that the choice of fission fragment distribution model has a strong effect on the final abundance distribution in r-process calculations. In our case, more elaborate and up-to-date models result in a better agreement with solar r-process abundances. This holds true for both extremely neutron-rich scenarios ($Y_e \approx 0.02 - 0.05$) like neutron star mergers and the moderately neutron-rich ($Y_e \approx 0.2 - 0.4$) jets of an MHD supernova.

Furthermore, we have shown that the nuclear mass model has a smaller impact than the fission distribution model. The ETFSI model tends to predict higher fission barriers compared to the FRDM model, i.e., the reaction path is allowed to run further. As a result, the fission products are heavier, which reflects in the second peak abundances.

We have also addressed the problem of the shifted third peak in NSM calculations. The shift is caused by neutron captures on heavy nuclei after the r-process freeze-out at a relatively low temperature ($T_9 < 1$) and a neutron density of around $n_n \approx 10^{15}$ cm^{-3}. To prevent this effect a higher temperature and/or a lower neutron density after the freeze-out is needed.

References

[1] Möller P, Nix J R, & Kratz K-L, At. Data Nucl. Data Tables **66**, 131 (1997).
[2] Rosswog S, Piran T, & Nakar E, MNRAS **430**, 2585 (2013).
[3] Korobkin O, et al., Mon. Not. R. Astron. Soc. **426**, 1940 (2012).
[4] Winteler C, et al., ApJ **750**, L22 (2012).
[5] Möller P, et al., At. Data Nucl. Data Tables **59**, 185 (1995).
[6] Aboussir Y, et al., At. Data Nucl. Data Tables **61**, 127 (1995).
[7] Myers W D & Swiatecki W J, Phys. Rev. C **60**, 014606 (1999).
[8] Mamdouh A, et al., Nucl. Phys. A **644**, 389 (1998).
[9] Petermann I, et al., Eur. Phys. J. A **48**, 122 (2012).
[10] Panov I V, Freiburghaus C, & Thielemann F-K, NuPhA **688**, 587 (2001).
[11] Kodama T & Takahashi K, NuPhA **239**, 489 (1975).
[12] Panov I V, Korneev I Yu, & Thielemann F-K, Astronomy Letters **34**, 189 (2008).
[13] Kelic A, et al., Proceedings: Dynamical Aspects of Nuclear Fission, World Scientific, p. 203 (2008) [Arxiv:0906.4193].
[14] Sneden C, Cowan J J, & Gallino R, ARA&A **46**, 241 (2008).